New Insights into Structures, Stability, and Bonding of μ-Allyl Ligands Coordinated with Pd−Pd and Pd−Pt Fragments

Hideo Kurosawa,* Kazuyoshi Hirako, Satoko Natsume, Sensuke Ogoshi, Nobuko Kanehisa, and Yasushi Kai

Department of Applied Chemistry, Osaka University, Suita, Osaka, Japan

Shigeyoshi Sakaki* and Kaori Takeuchi

Department of Applied Chemistry, Kumamoto University, Kumamoto, Japan

Received October 24, 1995[⊗]

A series of complexes of μ-allyl ligands coordinated with the Pd−Pd fragment $Pd_2(\mu\text{-allyl})(\mu\text{-Cl})(PPh_3)_2$ were prepared from reactions of the corresponding allylpalladium(II) chlorides with $Pd(C_2H_4)(PPh_3)_2$. The μ-allyl ligands employed contained both electron-withdrawing (Cl, CN, COOMe, SO_2Ph) and electron-donating (Me, Ph) substituents at either the terminal or central carbon of the allyl framework. The relative ability of a substituted allyl ligand to coordinate to the Pd(I)−Pd(I) fragment *vs* the mononuclear Pd(II) fragment was determined by means of an allyl ligand exchange equilibrium between the dinuclear and the mononuclear fragments. The allyl ligand bearing the more withdrawing substituent coordinated to the Pd−Pd fragment more strongly than that bearing the less withdrawing substituent. The 1-methyl, 1-phenyl, and 1-chloroallyl ligands on the Pd−Pd bond exist in an anti configuration almost exclusively. X-ray structure determinations of some of the μ-allyl Pd−Pd and Pd−Pt complexes, $PdM(\mu\text{-allyl})(\mu\text{-X})(PPh_3)_2$ (**11**, M = Pt, allyl = $CH_2C(COOMe)CH_2$, X = Br; **12**, M = Pd, allyl = $CH_2C(COOMe)CH_2$, X = Br; **13**, M = Pd, allyl = $CH_2CHCH(COOMe)$, X = SPh) were carried out. The crystal of **11** was isomorphous with that of **12**. The results revealed a unique geometrical feature of the bridging allyl ligand; the dihedral angle between the allyl plane and the approximate coordination plane (M−M−X plane) is smaller than 90°. Ab initio MO calculations on the model $Pd_2(\mu\text{-}CH_2CHCH_2)(\mu\text{-Br})(PH_3)_2$ were performed to reveal important aspects of the bonding nature; the coordinate bond of the μ-allyl ligand involved not only donation from the allyl nonbonding π orbital to the unoccupied dσ−dσ antibonding orbital of the $Pd_2(\mu\text{-Br})(PH_3)_2$ unit but also back-donation from the occupied dσ−dσ and dπ−dπ bonding combinations of the $Pd_2(\mu\text{-Br})(PH_3)_2$ unit to the allyl π* orbital. The latter is not observed in the mononuclear palladium(II) allyl complex but is found as a characteristic interaction in the dinuclear μ-allyl complex. The above-mentioned unique geometrical and stability features of the dinuclear μ-allyl complexes arise from the back-bonding interaction.

Increasing attention has been paid to structures and bonding of hydrocarbon ligands which coordinate to multinuclear metal centers in a bridging manner because of their close bearing with metal surface−hydrocarbon interaction models.[1] Several complexes of μ-allyl ligands bound on metal−metal fragments have beeen prepared,[2,3] and a simple view of their bonding nature was also presented.[2c,e,3d,f] However, it seems that little has been clarified concerning the bonding and structrual aspects intrinsic to the μ-allyl ligand, especially when these were compared with the aspects intrinsic to the extensively studied η^3-allyl ligand bound to mononuclear metal centers.[4] By mononuclear complex we mean those which contain no metal−metal bonds.

Werner and his co-workers have carried out extensive studies on synthesis and structures of μ-allyl complexes with Pd−Pd, Pd−Pt and Pt−Pt fragments,[3f] but the allyl ligands they employed were mostly restricted to those of a simple structure type such as unsubstituted

[⊗] Abstract published in *Advance ACS Abstracts,* March 15, 1996.

(1) (a) Beck, W.; Niemer, B.; Wieser, M. *Angew. Chem., Int. Ed. Engl.* **1993**, *32*, 923−1110 and references therein. (b) Wadepohl, H. *Angew. Chem., Int. Ed. Engl.* **1992**, *31*, 247−262. (c) Casey, C. P.; Audett, J. D. *Chem. Rev.* **1986**, *86*, 339−352. (d) Stone, F. G. A. *Angew. Chem., Int. Ed. Engl.* **1984**, *23*, 89−99. (e) Holton, J.; Lappert, M. F.; Pearce, R.; Yarrow, P. I. W. *Chem. Rev.* **1983**, *83*, 135−201.

(2) (a) Chihara, T.; Yamazaki, H. *J. Chem. Soc., Dalton Trans.* **1995**, 1369−1377. (b) *J. Organomet. Chem.* **1992**, *428*, 169−186. (c) Housecroft, C. E.; Johnson, B. F. G.; Lewis, J.; Lunnis, J. A.; Owen, S. M.; Raithby, P. R. *J. Organomet. Chem.* **1991**, *409*, 271−284. (d) Chihara, T.; Aoki, K.; Yamazaki, H. *J. Organomet. Chem.* **1990**, *383*, 367−385. (e) Chisholm, M. H.; Hampden-Smith, M. J.; Huffman, J. C.; Moodley, K. G. *J. Am. Chem. Soc.* **1988**, *110*, 4070−4071. (f) Bruce, M. I.; Williams, M. L. *J. Organomet. Chem.* **1985**, *288*, C55−C58.

(3) (a) Osakada, K.; Ozawa, Y.; Yamamoto, A. *J. Organomet. Chem.* **1990**, *399*, 341−348. (b) Osakada, K.; Chiba, T.; Nakamura, Y.; Yamamoto, T.; Yamamoto, A. *Organometallics* **1989**, *8*, 2602−2605. (c) Hayashi, Y.; Matsumoto, K.; Nakamura, Y.; Isobe, K. *J. Chem. Soc., Dalton Trans.* **1989**, 1519−1525. (d) Zhu, L.; Kostic, N. M. *Organometallics* **1988**, *7*, 665−669. (e) Sieler, J.; Helms, M.; Gaube, W.; Svensson, A.; Lindqvist, O. *J. Organomet. Chem.* **1987**, *320*, 129−136. (f) Werner, H. *Adv. Organomet. Chem.* **1981**, *19*, 155−182. (g) Kobayashi, Y.; Iitaka, Y.; Yamazaki, H. *Acta Crystallogr.* **1972**, *B28*, 899−906.

(4) (a) Collman, J. P.; Hegedus, L. S.; Norton, J.; Finke, R. G. *Principles and Applications of Organotransition Metal Chemistry*; University Science Books: Mill Valley, CA, 1987; p 175. (b) Curtis, M. D.; Eisenstein, O. *Organometallics* **1984**, *3*, 887−895.

0276-7333/96/2315-2089$12.00/0

and, at most, 2-alkyl-substituted allyls. Further, the supporting phosphine ligands in their studies, e.g. tricyclohexylphosphine, appear to us not suitable, in a sense, for a detailed ^{1}H NMR study through which more detailed knowledge with regard to the solution properties can be obtained. In order to gain a deep insight into the precise bonding nature between the μ-allyl ligand and the metal−metal fragment, it is necessary to synthesize a series of μ-allyl complexes which contain a wide variety of substituents at the allyl carbon and those supporting ligands that exhibit NMR spectroscopic features as simple as possible. We wish to describe here the synthesis of a series of complexes of μ-allyl ligands coordinated to the Pd−Pd and Pd−Pt fragments with PPh_3 as a supporting ligand and novel aspects of their solution stabilities and structures, both in the solid state and in solution. These features will be explained in terms of the unique nature of bonding between the μ-allyl ligand and the metal−metal fragment deduced from MO calculations.

Results

Synthesis of Complexes. According to the general procedure developed by Werner and co-workers,[3f] we synthesized a series of μ-allyl complexes of the Pd−Pd fragment containing a PPh_3 ligand, **1**−**9**, in moderate yields through reactions between (η^3-allyl)palladium(II) chlorides and a Pd(0)−ethylene complex (eq 1).

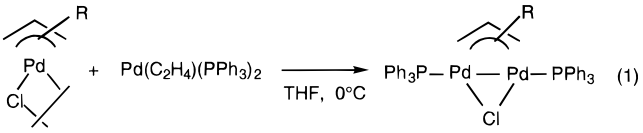

1 - **9**

1, R= H; **2**, R= 1-Me; **3**, R= 1-Ph; **4**, R= 1-COOMe; **5**, R= 1-Cl; **6**, R= 2-Cl; **7**, R= 2-COOMe; **8**, R= 2-CN; **9**, R= 2-SO_2Ph

The complexes containing electron-withdrawing substituents at the allyl carbon were somewhat easier to handle than the others, which when kept in solution at room temperature tended to decompose in a few hours. The Pd−Pd complexes of μ-allyl ligands containing electron-donating substituents at the center allyl carbon, $Pd_2(\mu\text{-}CH_2CRCH_2)(\mu\text{-}Cl)(PPh_3)_2$ (R = Me, OCH_2-PH), were difficult to isolate pure by eq 1 but were unambiguously characterized by ^{1}H NMR spectroscopy (see Experimental Section). The ^{1}H NMR spectra of all the complexes were straightforwardly interpreted; of particular note was the elucidation of the ratio of syn and anti isomers of the 1-substituted allyl derivatives (see later).

The reaction of *trans*-(5-(methoxycarbonyl)(1−3−η)-cyclohexenyl)palladium chloride[5] with the Pd−ethylene complex afforded a good yield of the corresponding dipalladium complex **10**, in which the $Pd_2(\mu\text{-}Cl)(PPh_3)_2$ moiety lies opposite to the COOMe group with respect to the cyclohexenyl ring, as comfirmed by NOE experiments. Thus, irradiation of the ortho proton signal of the P−Ph groups resulted in a 9% increase of the resonance attributable to the hydrogen geminal to the COOMe group. This retention of stereochemistry with regard to the allylic carbon upon reaction of $Pd(C_2H_4)(PPh_3)_2$ with $[Pd(\eta^3\text{-allyl})(Cl)]_2$ (allyl = *trans*-(5-(methoxycarbonyl)((1−3-η)-cyclohexenyl) is in marked contrast to the inversion of stereochemistry brought about by the exo attack of $Pd(C_2H_4)(PPh_3)_2$ at the allyl ligand in the cation $[Pd(\eta^3\text{-allyl})(PPh_3)_2]^+$.[6]

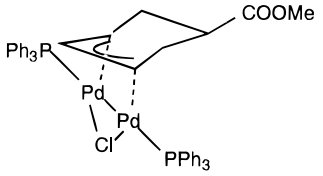

10

The reaction of an allylplatinum(II) complex containing a PPh_3 ligand with $Pd_2(dba)_3$ afforded a μ-allyl complex with the Pd−Pt bond, **11**, in 53% yield (eq 2).

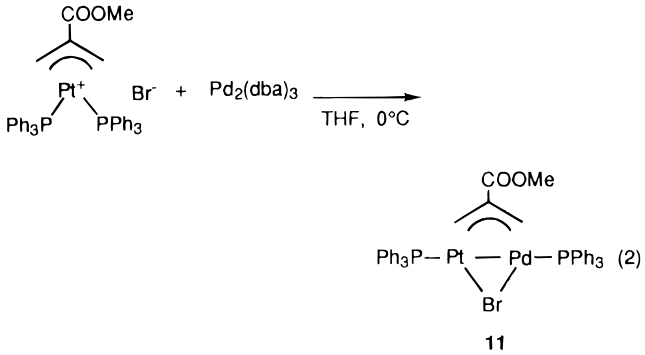

11

This was considerably stable even if left at room temperature both in the solid and in solution. Noteworthy here is that the reaction with the reverse combination, namely the reaction between the corresponding (2-(methoxycarbonyl)allyl)palladium(II) bromide and $Pt(C_2H_4)(PPh_3)_2$, did not lead to a satisfactory result; the desired heteronuclear complex was always contaminated by a comparable amount of the Pd−Pd analog $Pd_2[\mu\text{-}CH_2C(COOMe)CH_2](\mu\text{-}Br)(PPh_3)_2$ (**12**). We cannot explain why this is so.

X-ray Structure Determination. Crystals of **11** suitable for X-ray diffraction analysis were obtained and subjected to structure determination. In the crystals of **11**, Pd and Pt atoms were disordered in equivalent occupancy, so that the structure was solved by applying the atomic scattering factor of Sm, which has an electron number corresponding to an average of those of Pd and Pt atoms, for the scattering factor of the metal atoms. The structures of **12** and of the μ-SPh analog of **4**, $Pd_2[\mu\text{-}CH_2CHCH(COOMe)](\mu\text{-}SPh)(PPh_3)_2$ (**13**), prepared in a manner similar to eq 1, were also determined by the X-ray diffraction method. The structures of the three complexes are shown in Figures 1−3. Table 1 summarizes some relevant bond lengths and angles for these three complexes and, for comparison, $Pd_2(\mu\text{-}CH_2CHCH_2)(\mu\text{-}Cl)(PPh_3)_2$ (**1**), determined previously.[3e] The structures of the two μ-2-(methoxycarbonyl)allyl complexes containing the Pd−Pd bond (**12**) and the Pd−Pt bond (**11**) show almost identical geometrical parameters with regard to the M−allyl bonding. Comparison of the structure of **12** with the unsubstituted analog **1** also

(5) Kurosawa, H.; Kajimaru, H.; Ogoshi, S.; Yoneda, H.; Miki, K.; Kasai, N.; Murai, S.; Ikeda, I. *J. Am. Chem. Soc.* **1992**, *114*, 8417−8424.

(6) (a) Granberg, K. L.; Backvall, J. *J. Am. Chem. Soc.* **1992**, *114*, 6858−6863. (b) Kurosawa, H.; Ogoshi, S.; Chatani, N.; Kawasaki, Y.; Murai, S.; Ideda, I. *Chem. Lett.* **1990**, 1745−1748.

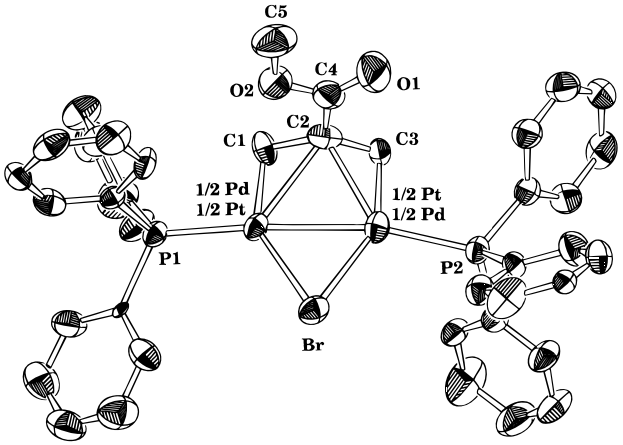

Figure 1. Molecular structure of **11** with thermal ellipsoids at 50% probability levels.

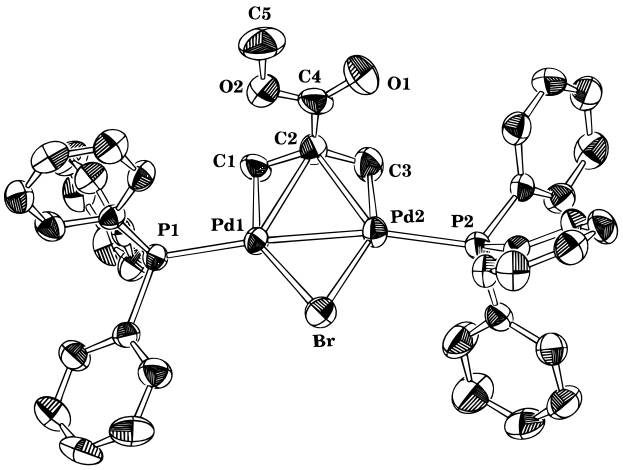

Figure 2. Molecular structure of **12** with thermal ellipsoids at 50% probability levels.

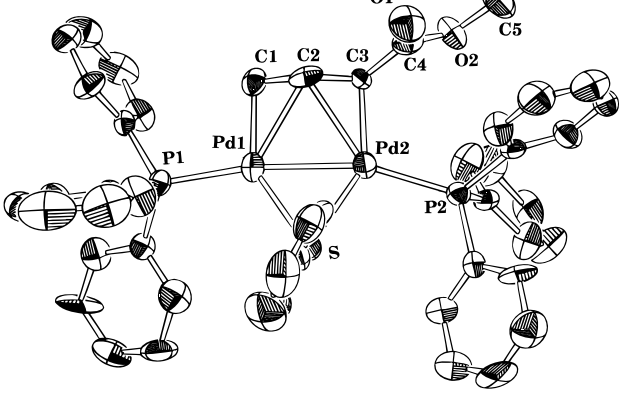

Figure 3. Molecular structure of **13** with thermal ellipsoids at 50% probability levels.

suggests very little geometrical difference between them except for somewhat longer C−C bonds of the allyl framework in **12** than those in **1**.

We emphasize some unique structure aspects common to the μ-allyl complexes of the Pd−Pd and Pd−Pt fragments which have received less attention in the related, previous structures studies[3a,c,e,f,g] but which we believe are key to understanding the metal−allyl bonding nature. These concern the spatial dispositions of some donor atoms relative to the M−M−X plane (X = Cl, Br, S), as summarized in Table 2. The data in the table include those for **1** which we recalculated by using the atomic coordinates reported.[3e] First, two terminal carbons (C_t) of the allyl ligand lie almost on the M−M−X plane, while in the mononuclear complexes they lie off the coordination plane with the center of gravity of the allyl triangle being on the coordination plane,[7] even though the vigorous definition of the coordination plane may be somewhat difficult in the dinuclear complexes. For example, the P atoms deviate from the M−M−X plane to some extent, in addition to the downward bending from the horizontal line connecting two metal atoms. Apparently these movements of the P atoms are due to repulsion between the phosphine and the allyl ligands.

Second, Table 2 shows that the dihedral angle (θ; Chart 1) between the allyl plane and the M−M−X plane is smaller than 90° where the allyl central carbon leans toward the M−M bond. In contrast, it is well-known that in mononuclear η^3-allyl complexes of Pd and Pt the allyl plane makes an angle larger than 110° with the metal coordination plane.[7] Thus, the direction of leaning of the allyl plane in the dinuclear μ-allyl complexes is opposite to that in the mononuclear η^3-allyl complexes.

Table 1. Relevant Bond Lengths (Å) and Angles (deg)[a]

	11	**12**	**13**	**1**[b]	MP2 calcd[c]
M−M	2.675(1)	2.642(1)	2.625(2)	2.623(1)	2.635 (2.636)[d]
M−C_t	2.05(1) 2.06(1)	2.075(7) 2.088(7)	2.07(2) 2.10(2)	2.07(1) 2.07(1)	2.115 (2.113)
M−C_c	2.38(1) 2.55(1)	2.421(7) 2.518(7)	2.43(2) 2.47(2)	2.45(1) 2.46(1)	2.518 (2.515)
M−X	2.531(1) 2.542(2)	2.5295(9) 2.537(1)	2.358(5) 2.371(5)	2.433(3) 2.438(3)	2.624 (2.624)
M−P	2.235(3) 2.251(3)	2.270(2) 2.284(2)	2.262(5) 2.279(4)	2.285(3) 2.287(3)	2.402 (2.398)
C_t−C_c	1.40(2) 1.46(2)	1.422(9) 1.435(9)	1.41(2) 1.41(2)	1.37(2) 1.40(2)	1.427 (1.427)
C_t−C_c−C_t	126(1)	123.3(8)	124(1)	133.7(9)	126 (126)
P−M−M	167.05(9) 173.65(9)	167.90(6) 173.58(6)	160.1(1) 167.5(1)	166.5(1) 173.0(1)	173 (172)
M−X−M	63.64(4)	62.88(3)	67.4(1)	65.2(1)	60 (60)

[a] C_t terminal carbon of allyl; C_c = center carbon of allyl. [b] Reference 3e. [c] MP2 calculation for $Pd_2(\mu\text{-}CH_2CHCH_2)(\mu\text{-}Br)(PH_3)_2$. [d] In parentheses: a triple-ζ basis function was used for d electrons of Pd without any other modification on the other basis functions.

Table 2. Atomic Deviations (Å) from the M−M−X Plane and Dihedral Angles (deg) between the M−M−X and Allyl Planes[a]

	11	**12**	**13**	**1**[b]	MP2 calcd[c]
C_t	0.019 −0.136	0.013 −0.187	0.010 0.023	0.042 −0.011	0.022 (0.023)[d]
C_c	0.584	0.585	0.645	0.551	0.669 (0.669)
P	−0.244 −0.357	−0.251 −0.351	−0.447 −0.539	−0.231 −0.456	−0.31 (−0.31)
θ	84.2	83.7	79.5	82.1	83 (83)

[a] C_t = terminal carbon of allyl; C_c = center carbon of allyl; θ = dihedral angle between M−M−X and C_t−C_c−C_t planes. [b] Calculated by using atomic coordinates reported in ref 3e. [c] MP2 calculation for $Pd_2(\mu\text{-}CH_2CHCH_2)(\mu\text{-}Br)(PH_3)_2$. [d] See footnote *d* of Table 1.

(7) (a) Maitlis, P. M.; Espinet, P.; Russell, M. J. In *Comprehensive Organometallic Chemistry*; Wilkinson, G., Stone, F. G. A., Abel, E. W., Eds.; Pergamon: New York, 1982; Vol. 6, Chapter 38.7. (b) Hartley, F. R. In ref 7a, Vol. 6, Chapter 39.

Chart 1

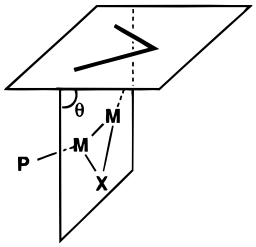

Table 3. Isomer Ratio of 1-Substituted Allyl Complexes in $CDCl_3$

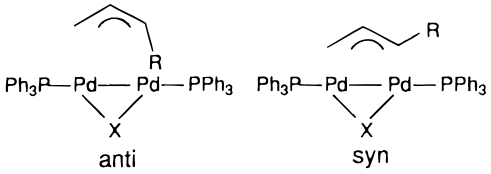

R	X	anti/syn	R	X	anti/syn
Me	Cl	97/3	Ph	Cl	100/0
Me	Br	96/4	Cl	Cl	100/0
Me	I	100/0	COOMe	Cl	21/79

Anti−Syn Isomerism in Solution. The ratios of the anti and syn isomers of 1-substituted μ-allylic complexes are summarized in Table 3. Intriguingly, these complexes showed a strong preference for the anti configuration, except for the 1-COOMe analog. All the configurations were unambiguously established on the basis of spin−spin coupling constants showing a larger value for the central proton−anti proton coupling than for the central proton−syn proton coupling. Moreover, the anti configurations of **2**, **3**, and **5** were also confirmed by NOE experiments; irradiation at the methyl resonance of the major isomer of **2** resulted in a 6% increase of the anti proton resonance at the other allyl end, and irradiation at the resonance for the proton geminal to the 1-Ph and 1-Cl substituents led to 7% and 12% increases of the central proton resonance, respectively.

The anti preference of complexes **2**, **3**, and **5** is in marked contrast to trends in mononuclear η^3-allyl systems;[8] for example, the corresponding complexes $[Pd(\eta^3\text{-}CH_2CHCHR)(Cl)]_2$ (R = Me, Ph, COOMe) existed in an almost exclusive syn form and the 1-chloro analog showed an anti/syn ratio of 11/89. The data in Table 3 correspond to those of thermodynamic origin, since an NMR monitoring of the reaction between $[Pd(\eta^3\text{-}CH_2CHCHCl)(Cl)]_2$ and $Pd(C_2H_4)(PPh_3)_2$ allowed the syn isomer of **5** to be detected at the early stages, which gradually isomerized to the anti isomer. A similar syn to anti isomerization has been found[3b] in the μ-1-methylallyl complex $Pd_2(\mu\text{-}CH_2CHCHMe)(\mu\text{-}SPh)(PCy_3)_2$, which likewise showed a high thermodynamic anti/syn ratio (90/10).

Allyl Ligand Exchange between Mono- and Dinuclear Complexes. When the (μ-allyl)dipalladium complexes were kept in contact with mononuclear allylpalladium(II) chloride complexes containing one PPh_3 ligand, facile allyl exchange took place as shown in eq 3. However, the reaction of each dinuclear complex with a half equimolar allylpalladium(II) chloride dimer led to decomposition of the former dinuclear complex into palladium metal, the remaining metal moiety being identified as $Pd(\eta^3\text{-allyl})(Cl)(PPh_3)$. Equilibration in eq 3 was complete within 5 min after mixing the substrates at 25 °C.

Table 4. Equilibrium Constants (K) of eq 3

R	K	R	K
1-Me	1.1×10^{-2}	1-Cl	1.2×10^{2}
1-Ph	1.7×10^{-1}	2-Cl	9.8
2-OCH_2Ph	9.2×10^{-3}	2-CN	1.4×10^{2}
2-Me	1.5×10^{-2}	2-COOMe	2.5×10^{2}
1-COOMe	1.5×10	2-SO_2Ph	3.6×10^{2}

^{1}H NMR resonances of the four complexes involved in the equilibrium can be separately discerned, suggesting that the rate of allyl ligand exchange is slower than the NMR time scale. Yet spin saturation transfer experiments on the system R = H in eq 3 qualitatively

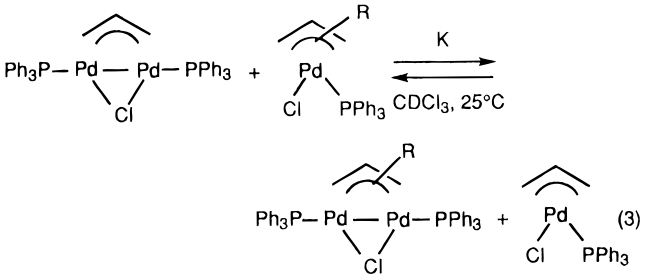

suggested the rate of allyl exchange to be on the order of ^{1}H spin relaxation time; irradiation at the resonance frequency for anti-H of **1** (δ 1.48) resulted in a decrease (ca. 16%) of the signals due to both anti and syn H of $Pd(\eta^3\text{-}CH_2CHCH_2)(Cl)(PPh_3)$ (δ 2.7−4.8). Such saturation transfer from anti to syn protons suggests that moderately fast syn−anti proton exchange in the complexes involved may also be taking place. Currently we cannot offer mechanisms of the allyl ligand exchange shown in eq 3.

Whatever the mechanism is, the substituent effect on the preferred coordination of an allyl ligand to the Pd−Pd fragment was deduced by taking advantage of such allyl group exchange. The equilibrium constant of eq 3 for a given R was determined as an average of more than three measurements, each measurement employing a different ratio of composites. The K values for several R substituents are summarized in Table 4, and a plot of log K against Hammett's σ parameter for a series of 2-substituted allyl complexes is shown in Figure 4.

Each point in Figure 4 shows no significant deviation from the least-squares line, suggesting a relatively insignificant steric effect of the substituent at the central carbon in determining the relative stability. Of particular note in Figure 4 is the large ρ value (4.76). Moreover, there was observed a closely related trend, with the 1-substituted analogues showing larger K values for the complexes having the more electron-withdrawing substituents, as shown in Table 4. These results suggest that the allyl ligand containing the electron-withdrawing substituent at both 1- and 2-positions of the allyl framework coordinates to the Pd−Pd fragment more strongly than the allyl ligand containing the electron-donating substituent does, while the allyl

(8) For a recent strategy to unusual anti complexes of mononuclear systems, see: (a) Sjogren, M.; Hansson, S.; Norrby, P. O.; Akermark, B.; Cucciolito, M. E.; Vitagliano, A. *Organometallics* **1992**, *11*, 3954−3964. (b) Ward, Y. D.; Villanueva, L. A.; Allred, G. D.; Payne, S. C.; Semones, M. A.; Liebeskind, L. S. *Organometallics* **1995**, *14*, 4132−4156.

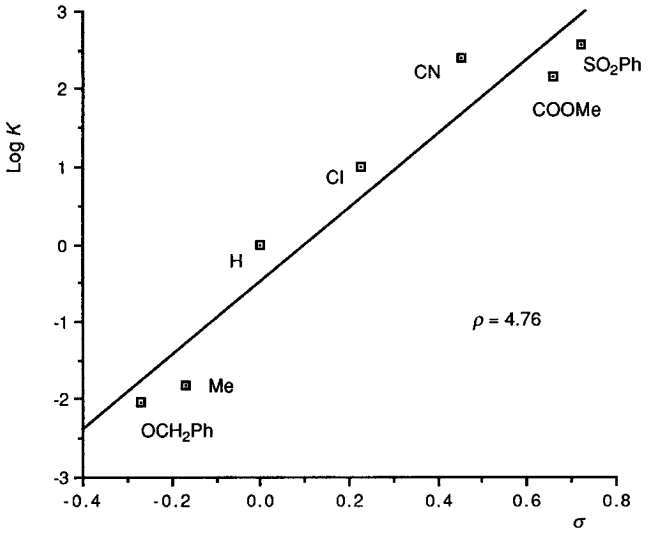

Figure 4. Plot of log K against Hammett σ constants for a series of 2-substituted allyl complexes. The σ value for the OCH_2Ph groups is replaced by that for the OCH_3 group.

ligand coordination to the mononuclear Pd(II) fragment might have a much diminished, if any, substituent dependency of similar trend or might be affected by the substituent in the reverse order. This situation is somewhat similar to the greater stability of electron-withdrawing olefin complexes of M(0) (M = Ni, Pd, Pt) with considerable electron flow from M to olefin, while M(II)−olefin complexes containing donating substituents at the olefin carbon are more stable than those of electron-withdrawing olefins.[9]

Ab Initio MO Calculations. The ab initio MO/MP2 calculations were performed on the model complex $Pd_2(\mu\text{-}CH_2CHCH_2)(\mu\text{-}Br)(PH_3)_2$. The optimized geometry of this model is also given in Tables 1 and 2. Although the calculated Pd−Br and Pd−P distances are longer than the experimental ones,[10] the calculated Pd−Pd, Pd−C_t, Pd−C_c, and C_t−C_c distances agree with experimental values. The dihedral angle between Pd−Pd−Br and allyl planes was calculated to be 83°.[11] This value is in good agreement with the experimentally observed value and is significantly smaller than the angle observed in mononuclear palladium(II) η^3-allyl complexes. MO calculations also showed that PH_3 was displaced from the Pd−Pd−Br plane by ca. 0.3 Å, like the experimental structure. From these results, it is reasonably concluded that the MP2 optimization can reproduce well the characteristic features of the bonding interaction between $\mu\text{-}CH_2CHCH_2$ and $Pd_2(\mu\text{-}Br)(PH_3)_2$.

It is also worthy of note that there is a clear contrast in the electron distribution between $Pd_2(\mu\text{-}CH_2CHCH_2)(\mu\text{-}Br)(PH_3)_2$ and $PdCl(\eta^3\text{-}CH_2CHCH_2)(PH_3)$; in the former the allyl ligand is considerably negatively charged (−0.23e), where the allyl radical is defined to have charge 0. In the mononuclear complex, however, the allyl ligand is much less negatively charged (−0.07e), indicating that the dinuclear complex involves weaker donation from ligand to metal and/or stronger back-donation from metal to ligand than the mononuclear complex. This feature would be related to the coordinate bond nature of $Pd_2(\mu\text{-}CH_2CHCH_2)(\mu\text{-}Br)(PH_3)_2$, as will be discussed below.

Chart 2

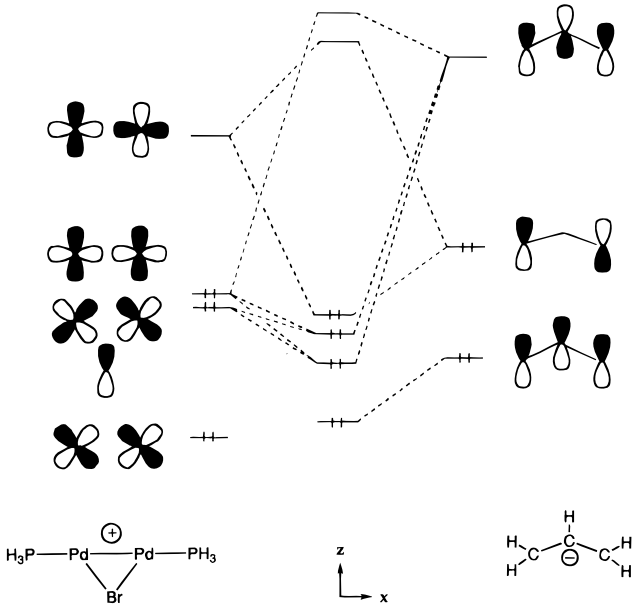

Discussion

The unique structure and solution stability of the dinuclear Pd μ-allyl complexes clarified in the present study can be nicely correlated with the nature of the metal−allyl bonding deduced from the ab initio MO calculations.

In an analysis of the coordinate bonding nature of the μ-allyl ligand, the present complex $Pd_2(\mu\text{-}CH_2CHCH_2)(\mu\text{-}Br)(PH_3)_2$ is considered to consist of $[Pd_2(\mu\text{-}Br)(PH_3)_2]^+$ and the allyl anion (Chart 2), as in many theoretical works.[2e,3d,4b] The allyl anion possesses the nonbonding π orbital (nπ) as its HOMO, the π orbital below the HOMO, and the π^* orbital as its LUMO. These orbitals play important roles in combining the allyl ligand with the Pd−Pd fragment. In $[Pd_2(\mu\text{-}Br)(PH_3)_2]^+$, the LUMO is the d$\sigma$−d$\sigma$ antibonding orbital, the next LUMO is the 5s−5s bonding orbital, the HOMO is the dσ−dσ bonding orbital, and the next HOMO is the dπ−dπ bonding orbital, into which the Br p_z orbital mixes in an antibonding way. The dπ−dπ antibonding orbital exists at a lower energy, because the Br p_z orbital cannot mix in it.

Of these orbitals, the dσ−dσ antibonding orbital (LUMO) overlaps well with the allyl nπ orbital (see Chart 2), when the C_t atoms lie on the coordination plane (Pd−Pd−Br plane). The next LUMO, a 5s−5s bonding orbital, also overlaps with the allyl π orbital, though to a lesser extent. These two interactions correspond to the donation from the allyl ligand to the Pd−Pd fragment. A similar bonding interaction has been proposed by Zhu and Kostic in the calculation of $Pd_2(\mu\text{-}CH_2CHCH_2)(\mu\text{-}Br)(PH_3)_2$.[3d] The allyl π^* orbital is in the a representation (C_s symmetry) and therefore overlaps with both the dσ−dσ bonding orbital (HOMO)

(9) Kurosawa, H.; Ikeda, I. *J. Organomet. Chem.* **1992**, *428*, 289−301.

(10) (a) The too long Pd−Br and Pd−P distances have been generally observed when the effective core potentials of Hay and Wadt were used with the split valence type basis set on P and halogen. Similar results were reported previously.[10b] Addition of the d polarization function to the ligand atoms considerably improves the optimized bond distance at the correlated level.[10c] (b) Low, J. J.; Goddard, W. A. *J. Am. Chem. Soc.* **1984**, *106*, 6928−6937. (c) Sakaki, S.; Satoh, H.; Shono, H.; Ujino, U. *Organometallics*, in press.

(11) This angle for the substituted complex $Pd_2[\mu\text{-}CH_2C(CN)CH_2](\mu\text{-}Br)(PH_3)_2$ was calculated to be 81°.

Chart 3

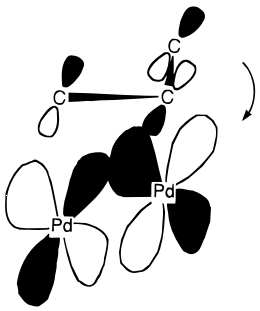

and the dπ−dπ bonding orbital to form a back-donating interaction from the Pd−Pd fragment to the allyl ligand. This interaction was neglected in the analysis by Zhu and Kostic,[3d] while Chisholm and co-workers proposed a similar interaction between the allyl π* and the W−W dπ−dπ bonding orbital in $W_2(\mu\text{-}CH_2CHCH_2)(NH_2)_4$.[2e] The geometrical feature of the dinuclear μ-allyl complexes cannot be explained successfully until we take into account both donating and back-donating interactions (see below). It should be noted that the geometry characteristic of the mononuclear complexes ($\theta > 90°$) is due to the occurrence of only the donating interactions from the allyl ligand to metals.[7b]

The terminal carbon atoms of the allyl group are fixed on the coordination plane so as to form the allyl nπ to metal LUMO donating interaction (see above) and to keep good overlap between the allyl π* and the dσ−dσ bonding orbitals. Therefore, only one possible geometry relaxation to yield a good overlap between the allyl π* orbital and the dπ−dπ bonding orbital is the leaning of the central carbon atom toward the Pd−Pd bond as shown in Chart 3. This geometry change decreases the dihedral angle between the allyl and Pd−Pd−Br planes to less than 90°. The important role of the back-bonding interaction is also well reflected in the electron distribution in the allyl ligand; the allyl ligand is considerably negatively charged in $Pd_2(\mu\text{-}CH_2CHCH_2)(\mu\text{-}Br)(PH_3)_2$ but much less negatively charged in $PdCl(\eta^3\text{-}CH_2CHCH_2)(PH_3)$. The back-donating interaction also explains the preferred coordination of those allyl ligands that contain the electron-withdrawing substituent at either the terminal or central carbon to the Pd−Pd fragment.

Rationalization of the unusual anti preference of the 1-substituted μ-allyl framework is somewhat difficult. In the 1-COOMe- and 1-Ph-substituted allyl moiety, electronically desirable π-conjugation would demand the substituent group to lie coplanar with the allyl plane, so that placing these substituents at the anti position would result in close contact between the anti 3-H of the allyl group and the oxygen (in COOMe) or ortho hydrogen (in Ph) atom. The structure of the 1-COOMe analog **4** or **13** thus can be attributable to the avoidance of such intraligand repulsions.

However, the preferred anti configuration of the 1-Ph analog must be explained by considering interligand repulsions more seriously. That is, the nearly linear arrangement of the $Ph_3P-Pd-Pd-PPh_3$ framework cannot accommodate the large 1-Ph substituent lying at the syn position. Examination of of the structure of **13** indicates that accommodation of the 1-COOMe group at the syn position is already just marginal in terms of the steric congestion, so that there is not enough room for the larger Ph substituent.

The origin of the anti preference of the rather small 1-Me and 1-Cl substituents in **2**, **5**, and their bromide or iodide analogues does not appear so straightforward. These substituents cannot necessarily lie on the allylic plane when located at the anti site, as was demonstrated in 1-substituted η^3-allyl complexes of Mo(II).[8b] This might lead us to propose a steric origin also for the anti preference of **2** or **5**, but we must await more comprehensive synthetic and X-ray structure studies on these and related complexes before deducing a definitive explanation including electronic, if any, origins.[12]

Concluding Remarks

Systematic examinations of structures and solution stabilities of a series of substituted μ-allyl complexes of Pd−Pd and Pd−Pt fragments enabled us to clarify the intrinsic metal−allyl bonding nature in metal−metal-bonded complexes. The observed structure and stability trends unique to the μ-allyl metal−metal complexes include a dihedral angle between the allyl and the coordination planes which is considerably smaller than in the mononuclear complexes, preferred coordination of the allyl ligand having electron-withdrawing substituents to the metal−metal fragment, and unusual anti configuration preference of the 1-substituted allyl ligand. These results, together with ab initio MO calculations, led us to offer an allyl−metal bonding scheme unique to the metal−metal complexes involving a greater degree of back-bond interaction from the Pd−Pd bond to the allyl π* orbital than in mononuclear Pd(II)−allyl complexes.

Experimental Section

Most of the commercially available reagents were used without further purification. All manipulations of dinuclear palladium complexes were carried out under an argon atmosphere by the use of standard vacuum-line techniques. Solvents were dried by standard methods and distilled prior to use. ^{1}H NMR spectra were obtained on JEOL GSX-270, JEOL GSX-400, and Bruker AM 600 spectrometers. Chemical shifts were referenced to internal TMS (^{1}H NMR) or external $P(OMe)_3$ (^{31}P NMR). Homodecoupling experiments were carried out, when necessary, to help in assigning spin−spin coupling patterns.

The following complexes were prepared according to the literature methods: $Pd(CH_2{=}CH_2)(PPh_3)_2$,[13] $[Pd(\eta^3\text{-}CH_2CHCHPh)(Cl)]_2$,[14] $[Pd(\eta^3\text{-}CH_2CHCHCOOMe)(Cl)]_2$,[15] $[Pd(\eta^3\text{-}CH_2CClCH_2)(Cl)]_2$.[16]

Preparation of $[PdCl(\eta^3\text{-}CH_2CHCHCl)]_2$. A mixture of $PdCl_2$ (1.0 g, 5.75 mmol) and LiCl (1.0 g, 23.6 mmol) was dissolved in 1 mL of water, followed by addition of 20 mL of THF and 1,3-dichloropropene (2.0 g, 18.0 mmol). Carbon monoxide was passed slowly under stirring through the

(12) (a) Notice that MO calculations of $[CH_2CHCHCH_3]^-$ and $[CH_2CHCHF]^-$ suggested the higher stability of the anti configuration than of the syn counterpart.[12b,c] (b) Schleyer, P. v. R.; Kaneti, J.; Wu, Y. D.; Chandrasekhar, J. *J. Organomet. Chem.* **1992**, *426*, 143−157 and references therein. (c) Tonachini, G.; Canepa, C. *Tetrahedron* **1989**, *45*, 5163−5174.

(13) Visser, A.; ven der Lind, R.; de Jongh, R. O. *Inorg. Synth.* **1976**, *16*, 127.

(14) Huttel, R.; Kratzer, J.; Bechter, M. *Chem. Ber.* **1961**, *94*, 766−780.

(15) Tsuji, J.; Imamura, S. *Bull. Chem. Soc. Jpn.* **1967**, *40*, 197−201.

(16) Lupin, M. S.; Powell, J.; Shaw, B. L. *J. Chem. Soc. A* **1966**, 1687−1691.

reddish brown solution for 3 h. The bright yellow solution obtained was dried by $MgSO_4$. Filtration of the solution and evaporation of the solvents under reduced pressure gave yellow solids which were washed with methanol and water and dried (929 mg, 74%). ^{1}H NMR ($CDCl_3$): syn isomer, δ 3.02 (d, J = 12.5 Hz, 1H, anti-H), 4.07 (d, J = 7.3 Hz, 1H, syn-H), 5.16 (d, J = 9.1 Hz, 1H, anti-H geminal to Cl), 5.75 (ddd, 1H, center-H); anti isomer, 4.03 (d, J = 12.9 Hz, 1H, anti-H), 4.47 (d, J = 7.7 Hz, 1H, syn-H), 5.42 (ddd, 1H, center-H), 5.93 (d, J = 4.6 Hz, 1H, syn-H geminal to Cl); syn/anti = 89/11. Mp: 148−149 °C dec. Anal. Calcd for $C_3H_4Cl_2Pd$: C, 16.58; H, 1.85. Found: C, 16.78; H, 1.85.

Preparation of [Pd(η^3-$CH_2C(COOMe)CH_2$)(Cl)]$_2$. In an argon-flushed, 500 mL round-bottomed flask equipped with a magnetic stirrer, a Dean−Stark trap, and a condenser were placed α-(bromomethyl)acrylic acid (7.0 g, 42 mmol) and 50 mL of benzene. Approximately 9 mL of a binary azeotrope of benzene and water was distilled. The Dean−Stark trap was removed, and 17 mL of absolute methanol and 0.17 mL of concentrated sulfuric acid were added slowly. The contents of the flask were boiled in an open atmosphere for 36 h, the condensate being passed through 15 g of molecular sieves (Linde 3A) before being returned to the flask. The reaction mixture was poured into 100 mL of water and neutralized with solid sodium bicarbonate until CO_2 evolution ceased. The resulting solution was extracted with three 13 mL portions of ether, and the combined extracts were dried over $MgSO_4$ for 6 h. The ether was removed under reduced pressure in a rotary evaporator, and the residues were distilled to give a fraction at 95 °C (0.1 mm) of methyl α-(bromomethyl)acrylate (2.06 g, 25%). ^{1}H NMR ($CDCl_3$): δ 3.70 (s, 3H), 4.13 (s, 2H), 5.91 (s, 1H), 6.28 (s, 1H). This was converted to [Pd(η^3-$CH_2CCOOMeCH_2$)(Br)]$_2$ using the standard method.[17] ^{1}H NMR ($CDCl_3$): δ 3.21 (s, 2H, anti-H), 3.89 (s, 3H, Me), 4.65 (s, 2H, syn-H). Mp: 167−170 °C dec. Anal. Calcd for $C_5H_7O_2BrPd$: C, 21.04; H, 2.47. Found: C, 21.52; H, 2.61.

The bromide was converted to the chloride on treatment with aqueous saturated ammonium chloride solution in CH_2Cl_2 for 24 h at room temperature. ^{1}H NMR ($CDCl_3$): δ 3.20 (s, 2H, anti-H), 3.87 (s, 3H, Me), 4.64 (s, 2H, syn-H). Mp: 157−158 °C dec. Anal. Calcd for $C_5H_7O_2ClPd$: C, 24.92; H, 2.93. Found: C, 24.69; H, 3.01.

Preparation of [Pd(η^3-$CH_2C(CN)CH_2$)(Cl)]$_2$. This was prepared from $PdCl_2$ and 2-cyano-3-chloro-1-propene (prepared from 2-cyano-3-hydroxy-1-propene[18] and $SOCl_2$ in HMPT) according to the standard method.[17] ^{1}H NMR ($CDCl_3$): δ 3.34 (s, 2H, anti-H), 4.44 (s, 2H, syn-H). Mp: 112−114 °C dec. Anal. Calcd for C_4H_4NClPd: C, 23.10; H, 1.94. Found: C, 23.59; H, 2.32.

Preparation of [Pd(η^3-$CH_2C(SO_2Ph)CH_2$)(Cl)]$_2$. This was prepared from 3-chloro-2-(phenylsulfonyl)-1-propene[19] and $PdCl_2$ by the standard method.[17] ^{1}H NMR (CD_3CN): δ 3.14 (s, 2H, anti-H), 4.21 (s, 2H, syn-H). Mp: 149−151 °C dec. Anal. Calcd for $C_9H_9SO_2ClPd$: C, 33.46; H, 2.81. Found: C, 33.39; H, 2.92.

Preparation of [Pd(η^3-$CH_2C(OCH_2Ph)CH_2$)(Cl)]$_2$. Reaction of $Pd_2(dba)_3$·$CHCl_3$ with a 5-fold excess of 3-chloro-2-(benzyloxy)propene, prepared by dehydrochlorination of 1,3-dichloro-2-(benzyloxy)propane[20] with potassium *tert*-butoxide, in CH_2Cl_2 afforded pale yellow solids. ^{1}H NMR ($CDCl_3$): δ 2.63 (d, J_H = 2.0 Hz, 2H, anti-H), 3.71 (d, J = 2.0 Hz, 2H, syn-H), 4.87 (s, 2H, OCH_2). Mp: 178 °C dec. Anal. Calcd for $C_{10}H_{11}OClPd$: C, 41.56; H, 3.84. Found: C, 41.46; H, 3.83.

Preparation of Pd_2(μ-allyl)(μ-Cl)(PPh_3)$_2$. General Procedure. To a THF solution (10 mL) of (η^3-allyl)palladium(II) chloride (0.15−0.25 mmol) was added an equimolar amount of $Pd(CH_2{=}CH_2)(PPh_3)_2$ at 0 °C. The reaction mixture immediately turned to a brown solution. After the solution was stirred for 10 min, the solvent was removed under reduced pressure at 0 °C. The residue was extracted with CH_2Cl_2. To the extract was added hexane, and this solution was kept in a refrigerator to give yellow solids.

Allyl = CH_2CHCH_2:[3e] yield, 60%; ^{1}H NMR (C_6D_6) δ 1.62 (d, J_H = 11.6 Hz, 2H, anti-H), 2.93 (m, J_H = 6.8, 11.6 Hz, J_P = 3.6 Hz, 1H, center-H), 3.07 (d of virtual t; J_H = 6.8 Hz, $J_P + J_{P'}$ = 12 Hz, 2H, syn-H).

Allyl = $CH_2CHCHMe$: yield, 31%. Anti isomer: ^{1}H NMR ($CDCl_3$) δ 0.40 (dd, J_H = 6.4 Hz, J_P = 4.1 Hz, 3H, anti-Me), 1.75 (dt, J_H = 2.3, 13.0 Hz, J_P = 2.3 Hz, 1H, anti-H), 2.64 (ddd, J_H = 2.3, 8.6 Hz, J_P = 10.8 Hz, 1H, syn-H), 2.89 (m, 1H, center-H), 3.57 (m, J_H = 6.4, 7.9 Hz, J_P = 12.1 Hz, 1H, syn-H geminal to Me); ^{31}P NMR ($CDCl_3$) δ −117.8 (d, J_P = 77 Hz), −116.3 (d). Syn isomer: ^{1}H NMR ($CDCl_3$) δ 1.12 (t, $J_H = J_P$ = 6.2 Hz, 3H, Me); mp 80−83 °C dec. Anal. Calcd for $C_{40}H_{37}P_2ClPd_2$: C, 58.03; H, 4.50. Found: C, 58.26; H, 4.77.

Allyl = $CH_2CHCHPh$: yield, 41%; ^{1}H NMR ($CDCl_3$) δ 1.94 (dt, J_H = 2.5, 13.0 Hz, J_P = 2.5 Hz, 1H, anti-H), 2.61 (ddd, J_H = 2.5, 8.4 Hz, J_P = 10.1 Hz, 1H, syn-H), 3.00 (m, 1H, center-H), 4.25 (dd, J_H = 9.5 Hz, J_P = 10.9 Hz, 1H, syn-H geminal to Ph); ^{31}P NMR ($CDCl_3$) δ −117.1 (d, J_P = 82 Hz), −113.8 (d); mp 128−130 °C dec. Anal. Calcd for $C_{45}H_{39}P_2ClPd_2$: C, 60.73; H, 4.42. Found: C, 60.80; H, 4.56.

Allyl = $CH_2CHCHCOOMe$: yield, 59%. Syn isomer: ^{1}H NMR (C_6D_6) δ 1.48 (dt, J_H = 2, 13.2 Hz, J_P = 2 Hz, 1H, anti-H), 2.81 (s, 3H, Me), 2.88 (ddd, J_H = 2, 8.4 Hz, J_P = 11.1 Hz, 1H, syn-H), 2.99 (dd, J_H = 11.4 Hz, J_P = 2.0 Hz, 1H, anti-H geminal to COOMe), 3.77 (m, 1H, center-H); ^{31}P NMR (C_6D_6) δ −118.0 (d, J_P = 84 Hz), −113.8 (d). Anti isomer: ^{1}H NMR (C_6D_6) δ 2.84 (s, 3H, Me), 3.19 (br d, J_H = 13.0 Hz, 1H, anti-H), 4.01 (t, $J_H = J_P$ = 8.5 Hz, 1H, syn-H geminal to COOMe); ^{31}P NMR (C_6D_6) δ −116.3 (d, J_P = 93 Hz), −113.7 (d); mp 146−147 °C dec. Anal. Calcd for $C_{41}H_{37}O_2P_2ClPd_2$: C, 56.48; H, 4.28. Found: C, 55.68; H, 4.35.

Allyl = $CH_2CHCHCl$: yield 72%; ^{1}H NMR ($CDCl_3$) δ 2.14 (dd, J_H = 12.1 Hz, J_P = 6.6 Hz, 1H, anti-H), 2.65 (t, $J_H = J_P$ = 8.7 Hz, 1H, syn-H), 2.86 (m, 1H, center-H), 4.96 (dd, J_H = 4.9 Hz, J_P = 17.5 Hz, 1H, syn-H geminal to Cl); ^{31}P NMR ($CDCl_3$) δ −116.8 (d, J_P = 79 Hz), −114.1 (d); mp 140−142 °C dec. Anal. Calcd for $C_{39}H_{34}P_2Cl_2Pd_2$: C, 55.21; H, 4.04. Found: C, 55.43; H, 4.21.

Allyl = CH_2CClCH_2: yield, 50%; ^{1}H NMR ($CDCl_3$) δ 1.76 (s, 2H, anti-H), 3.18 (br, 2H, syn-H); mp 138−142 °C dec. Anal. Calcd for $C_{39}H_{34}P_2Cl_2Pd_2$: C, 55.21; H, 4.04. Found: C, 55.02; H, 4.25.

Allyl = $CH_2C(COOMe)CH_2$: yield, 63%; ^{1}H NMR ($CDCl_3$): δ 1.42 (s, 2H, anti-H), 3.41 (virtual t, $J_P + J_{P'}$ = 11.6 Hz, 2H, syn-H), 3.56 (s, 3H, Me); mp 135−136 °C dec. Anal. Calcd for $C_{41}H_{37}O_2P_2ClPd_2$: C, 56.48; H, 4.28. Found: C, 56.73; H, 4.59.

Allyl = $CH_2C(CN)CH_2$: yield, 67%; ^{1}H NMR ($CDCl_3$) δ 1.41 (s, 2H, anti-H), 2.91 (br, 2H, syn-H); mp 142−146 °C dec. Anal. Calcd for $C_{40}H_{34}NP_2ClPd_2$: C, 57.27; H, 4.08. Found: C, 56.48; H, 4.23.

Allyl = $CH_2C(SO_2Ph)CH_2$: yield, 75%; ^{1}H NMR ($CDCl_3$) δ 1.50 (d, J_H = 4.5 Hz, 2H, anti-H), 3.08 (d of virtual t, J_H = 4.5 Hz, $J_P + J_{P'}$ = 11.0 Hz, 2H, syn-H); mp 175−179 °C dec. Anal. Calcd for $C_{45}H_{39}SO_2P_2ClPd_2$·$^1/_2CH_2Cl_2$: C, 54.84; H, 4.05. Found: C, 54.88; H, 4.24

The following complexes were prepared in a similar manner.

Pd_2[μ-$CH_2C(COOMe)CH_2$](μ-Br)(PPh_3)$_2$: yield, 55%; ^{1}H NMR ($CDCl_3$) δ 1.43 (s, 2H, anti-H), 3.50 (virtual t, $J_P + J_{P'}$ = 10.8 Hz, 2H, syn-H), 3.54 (s, 3H, Me); mp 140−145 °C dec. Anal. Calcd for $C_{41}H_{37}O_2P_2BrPd_2$: C, 53.74; H, 4.07. Found: C, 54.34; H, 3.99.

Pd_2[μ-$CHCHCHCH_2CH(COOMe)CH_2$](μ-Cl)(PPh_3)$_2$ (10): yield, 45%; ^{1}H NMR ($CDCl_3$) δ 1.1−1.3 (m, 4H, CH_2), 2.28 (tt, J_H = 3.5, 12.3 Hz, 1H, C*H*(COOMe)), 2.73 (m, 1H,

(17) Tatsuno, Y.; Yoshida, T.; Otsuka, S. *Inorg. Synth.* **1979**, *19*, 220−221.
(18) Villieras, J.; Rambaud, M. *Synthesis* **1982**, 924−926.
(19) Anzeveno, P. B.; Matthews, D. P.; Barney, C. L.; Barbuch, R. J. *J. Org. Chem.* **1984**, *49*, 3134−3138.
(20) Gu, X. P.; Ikeda, I.; Okahara, M. *Bull. Chem. Soc. Jpn.* **1987**, *60*, 397−398.

allyl-center), 3.47 (s, 3H, Me), 3.54 (br, 2H, allyl-terminal); mp 117−119 °C dec. Anal. Calcd for $C_{44}H_{41}O_2P_2ClPd_2$: C, 57.94; H, 4.53. Found: C, 56.67; H, 4.57.

^{1}H NMR Detection of $Pd_2[\mu$-$CH_2CRCH_2](\mu$-Cl)$(PPh_3)_2$ (R = Me, OCH_2Ph). These were formed in $CDCl_3$ according to eq 1.

R = Me: ^{1}H NMR ($CDCl_3$) δ 1.34 (t, J_P = 2.6 Hz, 3H, Me), 1.67 (s, 2H, anti-H), 2.98 (virtual t, $J_P + J_{P'}$ = 12.4 Hz, 2H, syn-H).

R = OCH_2Ph: ^{1}H NMR ($CDCl_3$) δ 1.66 (s 2H, anti-H), 3.07 (br, 2H, syn-H), 4.27 (s, 2H, OCH_2).

^{1}H NMR Monitoring of Reaction between $[PdCl(\eta^3$-$CH_2CHCHCl)]_2$ and $Pd(CH_2{=}CH_2)(PPh_3)_2$. To a $CDCl_3$ solution (0.5 mL) of $[PdCl(\eta^3$-$CH_2CHCHCl)]_2$ (2.2 mg; 0.01 mmol) in an NMR tube was added 6.9 mg (0.01 mmol) of $Pd(CH_2{=}CH_2)(PPh_3)_2$ at −78 °C. The tube was immediately placed at an NMR probe precooled to −80 °C. The temperature of the probe was raised to −40 °C within ca. 20 min, and ^{1}H NMR measurements showed resonances of the anti isomer of the dinuclear complex (43%) together with those for a supposedly syn isomer (25%): δ 1.30 (dd, J_H = 0.7, 14.0 Hz, anti-H), 4.12 (d, J_H = 9.0 Hz, anti-H geminal to Cl). The latter signal disappeared after the temperature was raised to room temperature, and instead, the former increased to 66% yield, with formation of the mononuclear complex $Pd(\eta^3$-$CH_2CHCHCl)Cl(PPh_3)$ (30%) also having been confirmed at the same time.

Preparation of $Pd_2(\mu$-$CH_2CHCHMe)(\mu$-X$)(PPh_3)_2$ (X = Br, I). These were prepared by reacting the corresponding chloride complex with excess LiX in CH_2Cl_2/acetone solution at 0 °C and recrystallized from CH_2Cl_2/*n*-hexane.

X = Br. Anti isomer: ^{1}H NMR ($CDCl_3$) δ 0.31 (dd, J_H = 6.0 Hz, J_P = 4.5 Hz, 3H, anti-Me), 1.77 (dt, J_H = 2.2, 12.9 Hz, J_P = 2.2 Hz, 1H, anti-H), 2.73 (ddd, J_H = 2.2, 8.5 Hz, J_P = 10.5 Hz, 1H, syn-H), 2.86 (m, 1H, center-H), 3.71 (m, J_H = 6.0, 6.3 Hz, J_P = 12.6 Hz, 1H, syn-H geminal to Me); ^{31}P NMR ($CDCl_3$) δ −115.0 (d, J_P = 84 Hz), −113.2 (d). Syn isomer: ^{1}H NMR ($CDCl_3$) δ 1.08 (t, $J_H = J_P$ = 6 Hz, 3H, Me); Mp 103−105 °C dec. Anal. Calcd for $C_{40}H_{37}P_2BrPd_2$: C, 55.07; H, 4.28. Found: C, 55.09; H, 4.68.

X = I: ^{1}H NMR ($CDCl_3$) δ 0.16 (dd, J_H = 6.3 Hz, J_P = 4.6 Hz, 3H, Me), 1.85 (dt, J_H = 2.0, 12.8 Hz, J_P = 2.0 Hz, 1H, anti-H), 2.86 (m, 1H, center-H), 2.94 (ddd, J_H = 2.0, 8.3 Hz, J_P = 9.9 Hz, 1H, syn-H), 4.04 (m, J_H = 6.3, 6.3 Hz, J_P = 12.3 Hz, 1H, syn-H geminal to Me); ^{31}P NMR ($CDCl_3$) δ −117.8 (d, J_P = 77 Hz), −116.3 (d); Mp 114−116 °C dec. Anal. Calcd for $C_{40}H_{37}P_2IPd_2$: C, 52.25; H, 4.06. Found: C, 51.90; H, 4.14.

Preparation of $Pd_2(\mu$-$CH_2CHCHCOOMe)(\mu$-SPh$)(PPh_3)_2$. $[Pd(\eta^3$-$CH_2CHCHCOOMe)Cl]_2$ (0.2 mmol, 48 mg) was dissolved in 5 mL of CH_2Cl_2 and cooled to 0 °C. TlSPh (0.22 mmol, 68 mg) was added to the solution. The reaction mixture was stirred for 4 h at 0 °C and was filtered, and the filtrate was concentrated to give orange solids (54 mg, 86%) of $[Pd(\eta^3$-$CH_2CHCHCOOMe)(SPh)]_2$. To a THF solution (5 mL) of this material (0.1 mmol, 31.4 mg) cooled to 0 °C was added $Pd(C_2H_4)(PPh_3)_2$ (0.1 mmol, 65.9 mg). The reaction mixture was stirred for 1 h at 0 °C and was concentrated. The residue was recrystallized from CH_2Cl_2/*n*-hexane to give yellow solids (52 mg, 55%). ^{1}H NMR ($CDCl_3$): δ 1.59 (d, J_H = 13.5 Hz, 1H, anti-H), 2.85 (s, 3H, Me), 3.10 (m, 2H, center-H and syn-H), 4.15 (m, 1H, anti-H geminal to COOMe). ^{31}P NMR ($CDCl_3$): δ −118.4 (d, J_P = 92.8 Hz), −114.0 (d). Mp: 130−133 °C dec. Anal. Calcd for $C_{47}H_{42}O_2P_2SPd_2{\cdot}CH_2Cl_2$: C, 55.94; H, 4.30. Found: C, 56.02; H, 4.48.

Preparation of PdPt$[\mu$-$CH_2C(COOMe)CH_2](\mu$-Br$)(PPh_3)_2$. Methyl α-(bromomethyl)acrylate (0.32 mmol, 224.3 mg) was added to a CH_2Cl_2 solution (5 mL) of $Pt(CH_2{=}CH_2)(PPh_3)_2$ (0.3 mmol, 224.3 mg) cooled to 0 °C. The reaction mixture was stirred for 2 h at 0 °C. The residue obtained upon evaporation of the solvent was recrystallized from CH_2Cl_2/*n*-hexane to give white soilds of $Pt[CH_2C(COOMe)CH_2](Br)(PPh_3)_2$ (216 mg, 80%). ^{1}H NMR (C_6D_6): δ 3.5 (br). Mp: 177−180 °C dec. Anal. Calcd for $C_{41}H_{37}O_2P_2BrPt{\cdot}CH_2Cl_2$: C, 51.29; H, 4.00. Found: C. 51.54; H, 4.35. To a THF solution (5 mL) of this material (0.1 mmol, 89.9 mg) was added $Pd_2(dba)_3{\cdot}CHCl_3$ (0.065 mmol, 67.3 mg). The reaction mixture was stirred for 20 min and was concentrated. The residue was purified by silica gel column chromatography with CH_2Cl_2 as eluent. The combined CH_2Cl_2 solution was concentrated and recrystallized from CH_2Cl_2/*n*-hexane to give yellow solids (53 mg, 53%). ^{1}H NMR ($CDCl_3$): δ 1.17 (br d, J_H = 5 Hz, J_{Pt} = 80 Hz, 1H, anti-H), 1.57 (s, 1H, anti-H), 2.98 (m, J_H = 5 Hz, J_P = 11.4 Hz, J_{Pt} = 88 Hz, 1H, syn-H), 3.52 (br d, J_P = 11.3 Hz, 1H, syn-H), 3.54 (s, 3H, Me). ^{31}P NMR ($CDCl_3$): δ −114.3 (d, J_P = 44.6 Hz, $^2J_{Pt}$ = 83.8 Hz), −109.5 (d, $^1J_{Pt}$ = 5928.6 Hz). Mp: 142−144 °C dec. Anal. Calcd for $C_{41}H_{37}O_2P_2BrPdPt{\cdot}CH_2Cl_2$: C, 46.28; H, 3.61. Found: C, 46.65; H, 3.67.

Allyl Ligand Exchange between the Dinuclear and Mononuclear Complexes. Substituted μ-allyl complexes were generated by adding the unsubstituted dinuclear complex $Pd_2(\mu$-$CH_2CHCH_2)(\mu$-Cl$)(PPh_3)_2$ (0.01 mmol) to a $CDCl_3$ solution (0.5 mL) of a 1- to 5-fold excess amount of (substituted (η^3-allyl)(triphenylphosphine)palladium(II) chloride, which was prepared from the corresponding (η^3-allyl)palladium chloride dimer and equimolar PPh_3. The NMR tube was set in a probe at 25 °C, and each component involved in eq 3 was integrated to give *K* values. Several measurements with different reagent ratios gave the averaged *K* values shown in Table 3.

Single-Crystal X-ray Diffraction Study. All data were obtained on a Rigaku AFC-5R diffractometer with graphite-monochromated Mo Kα radiation. All calculations were carried out with the TEXSAN crystallographic software package of Molecular Structure Corp. The structure was solved by direct methods and refined by full-matrix least-squares procedures, the function minimized being $\sum w(|F_o| - |F_c|)^2$. The non-hydrogen atoms were refined anisotropically. All the positions of the hydrogen atoms were calculated by stereochemical considerations.

PdPt$[\mu$-$CH_2C(COOMe)CH_2](\mu$-Br$)(PPh_3)_2$. A yellow crystal (0.3 × 0.3 × 0.3 mm) was obtained from CH_2Cl_2/*n*-hexane at −30 °C and was mounted on a glass fiber with epoxy resin: $C_{41}H_{37}BrO_2P_2PdPt{\cdot}CH_2Cl_2$, M_r = 1089.33, triclinic, space group $P\bar{1}$ *(No. 2)*, a = 13.534(2) Å, b = 14.142(3) Å, c = 11.676(3) Å, α = 111.40(2)°, β = 96.71(2)°, γ = 92.34(2)°, V = 2058.1(9) Å^3, Z = 2, D_{calc} = 1.758 g/cm^3, $F(000)$ = 1060, μ(Mo Kα) = 40.5 cm^{-1} by least-squares refinement on diffractometer angles from automatically centered reflections, 2θ range 27.3−27.5°, λ = 0.710 69 Å. The atomic scattering factor of Sm was used as the scattering factor of metal atoms. The final R and R_w values were 0.060 and 0.048, respectively, for 5505 reflections ($I > 3.00\sigma(I)$).

$Pd_2[\mu$-$CH_2C(COOMe)CH_2](\mu$-Br$)(PPh_3)_2$. A yellow crystal (0.3 × 0.45 × 0.2 mm) was obtained from CH_2Cl_2/*n*-hexane at −30 °C and was mounted on a glass fiber with epoxy resin: $C_{41}H_{37}BrO_2P_2Pd_2{\cdot}CH_2Cl_2$, M_r = 1001.33, triclinic, space group $P\bar{1}$ *(No. 2)*, a = 13.509(2) Å, b = 14.121(2) Å, c = 11.686(3) Å, α = 111.20(1)°, β = 97.03(2)°, γ = 92.30(2)°, V = 2054.3(7) Å^3, Z = 2, D_{calc} = 1.619 g/cm^3, $F(000)$ = 996, μ(Mo Kα) = 20.9 cm^{-1} by least-squares refinement on diffractometer angles from automatically centered reflections, 2θ range 27.3−27.5°, λ = 0.710 69 Å. The final R and R_w values were 0.047 and 0.045, respectively, for 6826 reflections ($I > 3.00\sigma(I)$).

$Pd_2[\mu$-$CH_2CHCHCOOMe](\mu$-SPh$)(PPh_3)_2$. A yellow crystal (0.3 × 0.2 × 0.2 mm) was obtained from CH_2Cl_2/*n*-hexane at −30 °C and was mounted on a glass fiber with epoxy resin: $C_{47}H_{42}O_2P_2Pd_2S{\cdot}H_2O$, M_r = 963.67, triclinic, space group $P\bar{1}$ *(No. 2)*, a = 14.278(2) Å, b = 15.815(3) Å, c = 10.281(3) Å, α = 106.12(2)°, β = 103.12(2)°, γ = 93.30(1)°, V = 2154.0(8) Å^3, Z = 2, D_{calc} = 1.486 g/cm^3, $F(000)$ = 976, μ(Mo Kα) = 9.98 cm^{-1} by least-squares reinement on diffractometer angles from automatically centered reflections, 2θ range 26.6−27.3°, λ = 0.710 69 Å. The final R and R_w values were 0.081 and 0.061, respectively, for 4000 reflections ($I > 3.00\sigma(I)$).

MO Calculations. Geometry optimization was carried out at the MP2 level with the following basis sets.[21] Core electrons of Pd (up to 3d) were replaced with effective core potentials, and valence electrons were represented with a (5s 5p 4d)/[3s 3p 2d] set.[22] For P and Br atoms, split valence basis sets (3s 3p)/[2s 2p][23] were adopted with ECPs used to replace core electrons. For C and H atoms, MIDI-3[24] and (4s)/[2s][25] sets were employed, where one d-polarization function was added to the C basis set. The geometry of PH_3 was taken from the experimental structure of the free PH_3 molecule.[26] All the calculations were performed with the Gaussian 92 program.[27]

Acknowledgment. Thanks are due to the Analytical Center, Faculty of Engineering, Osaka University, for the use of NMR facilities. Partial support of this work through Grants-in-aid for Scientific Research from the Ministry of Education, Science and Culture and Asahi Glass Foundation is also acknowledged.

Supporting Information Available: Tables of positional and thermal parameters and bond lengths and angles, together with figures giving atom-numbering schemes for **11**−**13** (29 pages). Ordering information is given on any current masthead page.

OM950843C

(21) The HF optimization of $Pd_2(\mu\text{-Br})(PH_3)_2(\mu\text{-}C_3H_5)$ gives rise to a somewhat larger dihedral angle (87°), which is larger than the MP2-optimized value by about 4°. The use of a basis set including no polarization function also yields a slightly larger dihedral angle (86°) even at the MP2 level. A method of quality higher than the MP2 optimization with a basis set including a d-polarization function would yield reasonable dihedral angle. Sakaki, S.; Kurosawa, H. To be submitted for publication.

(22) Hay, P. J.; Wadt, W. R. *J. Chem. Phys.* **1985**, *82*, 299−310.

(23) Wadt, W. R.; Hay, P. J. *J. Chem. Phys.* **1985**, *82*, 284−298.

(24) Huzinaga, S.; Andzelm, J.; Klobkowski, M.; Radio-Andzelm, E.; Sakaki, Y.; Tatewaki, H. *Gaussian Basis Sets for Molecular Calculations*; Elsevier: Amsterdam, 1984.

(25) Dunning, T. H.; Hay, P. J. In *Methods of Electronic Structure Theory*; Shaefer, H. F., Ed.; Plenum: New York, 1977; p 1.

(26) Herzberg, G. *Molecular Spectra and Molecular Structure*; Academic Press: New York, 1974; Vol. 3, p 267.

(27) Frisch, M. J.; Trucks, G. W.; Head-Gordon, M.; Gill, P.; M. W.; Wong, M. W.; Foresman, J. B.; Johnson, B. G.; Schlegel, H. B.; Robb, M. A.; Replogle, E. S.; Gomperts, R.; Andres, J. L.; Raghavachari, K.; Binkley, J. S.; Gonzalez, C.; Martin, R. L.; Fox, D. J.; DeFrees, D. J.; Baker, J.; Stewart, J. J. P.; Pople, J. A. Gaussian 92; Guassian Inc., Pittsburgh, PA, 1992.